Received: Added at production | Revised: Added at production | Accepted: Added at production

DOI: xxx/xxxx

ARTICLE TYPE

# Neural-Network-based Event-triggered Adaptive Security Path Following Control of AGVs Subject to Abnormal Actuator Signal

Hong-Tao Sun[1,2] | Pengfei Zhang[1] | Chen Peng*[2]

[1]School of Engeering, Qufu Normal University, Rizhao, Shandong, China
[2]School of Mechatronic Engineering and Automation, Shanghai University, Shanghai, China

**Correspondence**
C. Peng, Shanghai Key Laboratory of Power Station Automation Technology, and the Department of Automation, School of Mechatronic Engineering and Automation, Shanghai University, Shanghai, 200444, China. Email: c.peng@shu.edu.cn

**Abstract**

The malicious physical attacks from both sensor and actuator side make real threats to the security and safety of autonomous ground vehicles (AGVs). This paper focuses on the problem of neural-network-based event-triggered adaptive security control (ET-ASC) scheme for path following of AGVs subject to arbitrary abnormal actuator signal. Firstly, we assume that an arbitrary abnormal signal is caused by arbitrary malicious attacks or disturbances from actuators. Then, radial basis function neural network (RBF-NN) is used to reconstruct such abnormal actuator signal. Secondly, modelling issues on security path following control of AGVs with Sigmoid-like ETC scheme are shown when the AGV is suffering from abnormal actuator signal. In what follows, an ET-ASC scheme is developed to mitigate the adverse effects of abnormal actuator signal with the reconstructed abnormal signal based on a novel Sigmoid-like event-triggered communication scheme. By using the proposed RBF-NN-based ET-ASC scheme, $H_\infty$ control performance can be guaranteed under arbitrary malicious actuator signal rather than such attacks following a specific probability distribution. Finally, some simulation experiments are provided to verify the effectiveness of proposed ET-ASC scheme.

**KEYWORDS:**
event-triggered control, security control, actuator attacks, neural network, autonomous ground vehicle

## 1 | INTRODUCTION

Autonomous ground vehicles (AGVs) have drawn considerable attention over the past decade because its widespread applications in many promising areas such as self-driving, military mission.[1] As we all know, the introduction of in-vehicle network, i.e., CAN bus, leads vehicle dynamics to a typical networked control systems (NCSs). This brings many new challenges in the studies of AGVs.

Although various control problems have been investigated for the AGVs, the stability of path following control still becomes a hot topic because it is a fundamental issue in vehicle body control[2]. In fact, the stability for path following control of AGVs are depended on various factors such as network transmission, control algorithm and so on. So far, many different control strategies have been put forward to handle these issues, for example, a Stackelberg game theory is introduced to improve the stability and robustness of designed controller in order to guarantee optimal performance for vehicle path tracking[3], a path-planning approach based on the virtual potential field theory to seek the minimum incidence for collision on roads is investigated in Reference[4], a LMI-based MPC path-tracking controller is designed to against the vehicle time-varying speed and limit the tracking error into

an accepted magnitude[5]. The above researches are mainly focused on pursuit of advanced control algorithm, but the in-vehicle network factors are rarely considered.

*The first motivation of this paper lies that communication resources saving should be taking into consideration due to limited bandwidth of CAN bus.* All kinds of sensors and actuators, huge amounts of electronic control units (ECUs), and other smart devices are communicated via CAN bus. However, the maximum useful network bandwidth of the CAN bus is only around 296 Kbps[6]. In this instance, network congestion, which leads to the degrade quality of service (QoS) of CAN bus such as large time delay, packet dropouts, will have adverse effects on path following control performance of AGVs. Therefore, how to save communication resources in path following control of AGVs is crucial. Recently, the event-triggered communication scheme is developed to achieve minimum resource utilization, which is very different from the traditional NCSs are working in a time-triggered manner[7]. For example, a discrete ETC based on time-delay system theory was proposed[8,9]; the adaptive ETC schemes, which can adjust event-triggered threshold in an adaptive way, are developed in References[10,11]; a dynamic ETC scheme, which adjusts the event-triggered threshold by adding designed internal dynamics, is proposed in Reference[12]; a memory-based ETC scheme is proposed to improve robustness of transmission in Reference[13] proposed; a learning-based ETC scheme, which is similar to adaptive ETC scheme, is presented in Reference[14]. However, all the above vary-threshold ETC schemes are often designed in a complicated way and not easy to follow.

*The second motivation of this paper originated from that the vulnerability of CAN bus make a real threat to the path following control of AGVs.* In fact, CAN bus is still less IT protections under opening networked environments. Thus the control actions are easy to be affected by such as DoS attacks[15,16], deception attacks[17,18] and so on besides the vulnerability of the network itself. These potential threats lead to the controlled vehicle deviates significantly from the desired path and even causes accident on the road[19]. In recent years, security control for the NCSs have been drawn more and more attentions from both IT and control societies. For instance, a considerable amount of researches on cyber attacks have been carried out[20,21]. In Reference[22], a modified estimator is used to detect and estimate the deception attack on local vehicles in a platoon. Several detection algorithms for different kinds of false data injection attacks were detailed surveyed in Reference[23]. In fact, a malicious attacks, as well as disturbance from interior and external of vehicles, do not follow any determined rules such as periodicity, probability distribution, and so on. Therefore, a more generalized security strategies for arbitrary abnormal signal should be developed.

RBF-NN can approximate any continuous function with arbitrary precision and it is widely exploited owing to its good approximation ability and simple structure[24]. Thus, RBF-NN is often explored in nonlinear control design or estimate an unknown function. A neural-network-based state observer is designed to recover the damaged system states due to the influence of DoS attacks[25]. The RBF-NN approach is exploited to detect different cyber attacks[26]. An improved ErrCor algorithm is equipped with RBF-NN and it is applied to wastewater treatment process[27]. From the above analysis, if the malicious attacks signal can be estimated by such data-driven-based RBF-NN, then it can be well dealt with by model-based control approach. However, such intelligent algorithms are not included in the present security control strategies.

Motivated by the above discussions, this paper attempts to develop a RBF-NN-based event-triggered adaptive security control scheme for path following of AGV in order to cope with the adverse effects caused by abnormal actuator signal. The main contributions of this work can be summarized as follows

1. A Sigmoid-like ETC scheme is proposed to reduce transmissions for path following control of AGVs in an adaptive way. Compared with static ETC scheme (constant threshold)[28] and other complicated adaptive ETC schemes[10,11] or dynamic ETC schemes[12], the proposed Sigmoid-like ETC scheme shows a more brief formulation which the event-triggered threshold is adaptively adjusted according to the measurements directly.

2. RBF-NN-based ET-ASC scheme is used to mitigate the adverse effects caused by abnormal actuator signal. Different from the most existing works[13,14,18], which the specific probability distributions should be learned in advance, the developed ET-ASC scheme can be used to deal with arbitrary abnormal actuator signal caused by malicious attacks or/and disturbances where such arbitrary abnormal signal is reconstructed by RBF-NN.

The remainder of this paper is organized as follows. Modelling issues on path following control of AGVs with Sigmoid-like ETC subject to abnormal actuator signal are shown in Section 2. Main results regarding stability analysis and control synthesis of the attacked networked path following control with adaptive RBF-NN update law are presented in Section 3. Simulation results are shown in Section 4 and Section 5 concludes this paper.

*Notations:* $\mathbb{N}$ and $\mathbb{R}$ represent positive integers and real numbers, respectively. $\mathbb{R}^q$ denotes $q$-dimensional Euclidean space; $||\cdot||$ denotes the Euclidian norm for vectors; diag$\{\cdots\}$ denotes block-diagonal matrix; $X > 0$ represents positive definite matrix; $X^{\mathrm{T}}$ and $X^{-1}$ denote as the transpose and inverse of matrix $X$; $*$ stands for a symmetry term in a symmetric matrix.

**TABLE 1** Physical meanings of path following of AGVs

| Symbol | Meaning |
|---|---|
| $M$ | Vehicle mass |
| $CG$ | Center gravity of vehicle |
| $C_f$ | Front tire cornering stiffness |
| $C_r$ | Rear tire cornering stiffness |
| $F_{yf}$ | Lateral forces of the front tire |
| $F_{yr}$ | Lateral forces of the rear tire |
| $\alpha_f$ | Tire slip angle of the front tire |
| $\alpha_r$ | Tire slip angle of the rear tire |
| $\delta_f$ | Front wheel steering angle |
| $v_x$ | Longitudinal velocities |
| $v_y$ | Lateral velocities |
| $\phi_e$ | Heading error |
| $\phi_d$ | Tangential direction of the desired path |
| $I_z$ | Yaw rate of the vehicle |
| $e_l$ | Lateral offset |

## 2 | PRELIMINARIES AND PROBLEM FORMULATION

The interested on networked path following control of AGVs is described by Fig. 1 where the vehicle's sensors, electronic control units (ECUs) and actuators are exchanged information through CAN bus. Suppose that the attackers or other destroy sources launch their malicious attack or/and disturbance signal at the actuators. In this section, a sampled-data path following control framework for AGVs is formulated subject to networked introduced factors which included time delay, bandwidth limitation and security issues at the first subsection. Then the key idea of RBF-NN-based ET-ASC scheme and security control objectives are presented in the following subsections.

### 2.1 | Dynamics of Path Following Control Under Networked Environments

The path following model is shown in Fig. 2 and the symbols therein are explained in TABLE 1. The dynamic model is formulated in terms of lateral offset $e_l$ and heading error $\phi_e$ (between the AGV and the desired path), and the detailed kinetic equation is omitted in this paper. By defining as $x(t) = [e_l, \dot{e}_l, \phi_e, \dot{\phi}_e]^T$ the state vector, $\delta_f$ the control signal $u(t)$, $\dot{\phi}_d$ the road disturbance $w(t)$, the state space equation can be written as

$$\dot{x}(t) = Ax(t) + Bu(t) + B_\omega w(t) \tag{1}$$

where

$$A = \begin{bmatrix} 0 & 1 & 0 & 0 \\ 0 & -\frac{2C_f+2C_r}{Mv_x} & \frac{2C_f+2C_r}{M} & \frac{-2C_f l_f+2C_r l_r}{Mv_x} \\ 0 & 0 & 0 & 1 \\ 0 & \frac{-2C_f l_f+2C_r l_r}{I_z v_x} & \frac{2C_f l_f-2C_r l_r}{I_z} & -\frac{2C_f l_f^2+2C_r l_r^2}{I_z v_x} \end{bmatrix},$$

$$B_\omega = \begin{bmatrix} 0 & (\frac{-2C_f l_f+2C_r l_r}{Mv_x} - v_x) & 0 & -\frac{2C_f l_f^2+2C_r l_r^2}{I_z v_x} \end{bmatrix}^T,$$

$$B = \begin{bmatrix} 0 & \frac{2C_f}{M} & 0 & \frac{2C_f l_f}{I_z} \end{bmatrix}^T.$$

The following expressions are given to simplify the presentation of sampled-data-based path following control framework for AGVs.

1. The sensors are sampling at a fixed period $h$, then the sampled-data set is $S_1 = \{0, h, 2h, \cdots, kh\}$, $k \in \mathbb{N}$.

2. The sampled-data whether sent or not is depended on the designed communication scheme. Then the transmitted packets are defined as the set $S_2 = \{0, t_1h, t_2h, \cdots, t_kh\} \subseteq S_1, t_k \in \mathbb{N}, \lim_{k\to\infty} t_k \to \infty$.

3. The discreted control signals with zero-order-hold (ZOH) are further represented by the holding intervals $t \in [t_kh + \tau_k, t_{k+1}h + \tau_{k+1})$, where $\tau_k$ is the transmission delay, $t_kh + \tau_k$ is the instant when the control signal arrives at ZOH.

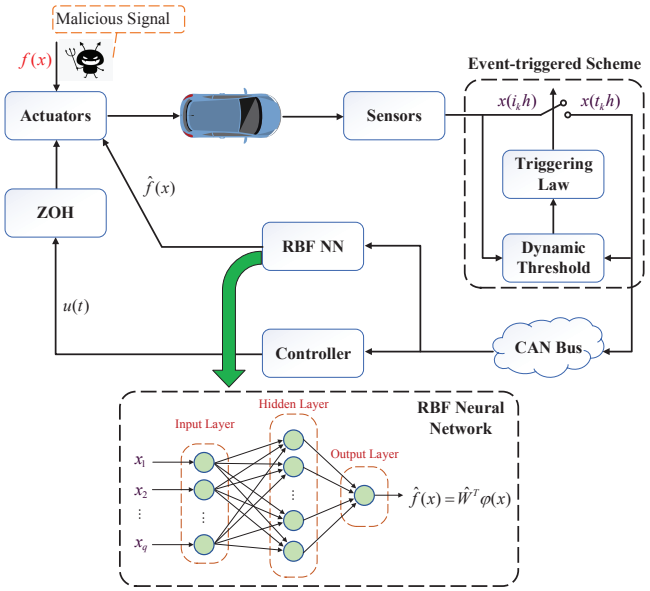


**FIGURE 1** ET-ASC structure of AGV under abnormal actuator signal.

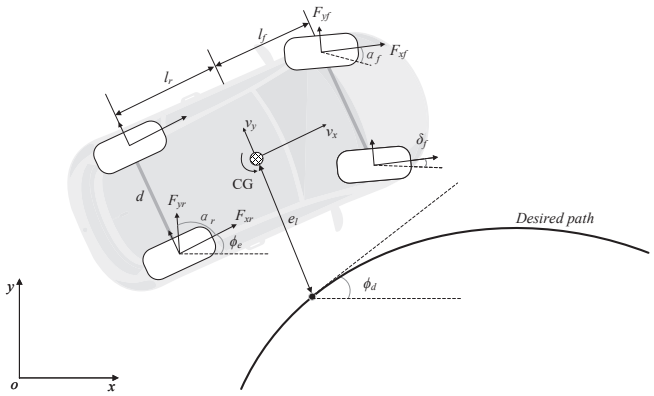


**FIGURE 2** Vehicle dynamic model with path tracking.

As depicted in Fig. 1, the control actions implemented by actuators are often disrupted by malicious attacks and disturbances. Suppose that the abnormal actuator signal is $f(x(t)) : \mathbb{R}^q \to \mathbb{R}$. For convenience, $f(x(t))$ is abbreviated as $f(x)$ hereafter. Then, in case of the abnormal actuator signal, the actual control actions can be written as

$$u^s(t) = u(t_kh) + f(x), t \in [t_kh + \tau_k, t_{k+1}h + \tau_{k+1}). \tag{2}$$

where $u(t_kh) = Kx(t_kh)$ follows a state feedback control form.

Combining the dynamics of system (1), the networked path following control of AGV can be formulated as

$$\begin{cases} \dot{x}(t) = Ax(t) + Bu^s(t) + B_\omega w(t) \\ y(t) = Cx(t) \\ u^s(t) = Kx(t_k h) + f(x), t \in [t_k h + \tau_k, t_{k+1} h + \tau_{k+1}) \end{cases} \tag{3}$$

where $u^s(t)$ is the control signal suffers abnormal actuator signal, and $y(t)$ is the measured outputs ($e_l$ and $\phi_e$ are the measured state).

*Remark 1.* As a special case, when $S_1 = S_2$, it means all the sampled-data are transmitted, i.e., the event-triggered communication scheme will become a time-triggered-based communication scheme with a fixed sampling period $h$[7].

*Remark 2.* It is worth noting that we do not make any specific assumptions on the malicious signal $f(x)$. However, numerous attacks are difficult to learn. Thus, the assumption on $f(x)$ in this paper is more practical than the works[26,27] which a specific probability distributions should be given at first.

## 2.2 | Sigmoid-like Event-triggered Communication Scheme

The part of 'Event-triggered Scheme' in Fig. 1 is described in this subsection. First, we propose a Sigmoid-like event-triggered communication (ETC) scheme as follows

$$t_{k+1} h = t_k h + \min_n \{nh | e^T(nh) \Phi e(nh) \geqslant S(t_k h) x^T(t_k h) \Phi x(t_k h)\}, \tag{4}$$

where $S(t_k h)$ is a dynamic triggered threshold whose value is dynamically adjusted online with $x(t_k h)$ according to the updating law

$$S(t_k h) = \frac{\phi_{\sigma,\vartheta}}{\sigma + \vartheta \cdot exp(\|x(t_k h)\|)} \tag{5}$$

with $\sigma$, $\vartheta$ and $\phi_{\sigma,\vartheta}$ are designed positive triggered parameters, which will be detailed later; $e(nh) = x(i_k h) - x(t_k h)$, $x(t_k h)$ is the last transmitted sampled-data, $x(i_k h)$ is the current sampled-data, $i_k h = t_k h + nh$, $n \in \mathbb{N}$, $h$ is the sampling period; $\Phi$ is a positive definite matrix to be designed.

It should be noted that a smaller triggered threshold in ETC scheme will leads to high frequency of invoked data transmissions and vice versa[29]. Thus, a well-designed Sigmoid-like ETC scheme is elaborated as follows

1. The threshold $S(t_k h)$ determines the frequency of the sampled-data transmissions, i.e., when the AGV deviates from the desired path, $S(t_k h)$ decreases gradually with the increasing of $\|x(t_k h)\|$, thereby the scheme (4) releases more data packets into controller and the system performance will be greatly enhanced. On the contrast, if the system reaches a stable state, i.e. following the desired path with a satisfied performance, a fewer number of packets are transmitted over the network.

2. The co-design of $\sigma$, $\vartheta$ and $\phi_{\sigma,\vartheta}$ make great differences on the sensitivity of Sigmoid-like ETC such that the transmission rate of the sampled-data can be scheduled in a more resource-efficient manner.

*Remark 3.* As a special case, if $\|x(t_k h)\| \to \infty$ in (5), it can be seen that $S(t_k h) \to 0$ in (4) and the event-triggered scheme (4) becomes a time-triggered communication scheme[7], i.e., $t_{k+1} h = t_k h + h$. Furthermore, if $\|x(t_k h)\| = 0$, the proposed Sigmoid-like ETC scheme degenerates into the static ETC[28] and its triggered threshold is constant $S(t_k h) = \frac{\phi_{\sigma,\vartheta}}{\sigma+\vartheta}$. In addition, the proposed discrete-time event-triggered scheme can guarantee the minimal inter-event time not less than one sampling period $h$ under the sampled-data-based control framework[30], therefore, the Zeno phenomenon is naturally excluded in this paper.

## 2.3 | RBF-NN Approximation

The part of 'RBF-NN' in Fig. 1 is described in this subsection. It is worth noting that RBF-NN has a capability to approach arbitrary continuous functions with arbitrary precision. Then, we can use the designed RBF-NN to approximate the malicious actuator signal $f(x)$.

Thus, the evaluated function $f(x)$ is described as

$$f(x) = W^{*T} \varphi(x) + \varepsilon, x \in \Omega \subset \mathbb{R}^q, \tag{6}$$

and the outputs of RBF-NN is given as

$$\widehat{f}(x) = \widehat{W}^T \varphi(x), \tag{7}$$

where $\varepsilon$ is the approximation error which satisfies $|\varepsilon| \leq \overline{\varepsilon}$, here, $\overline{\varepsilon}$ is a positive constant; $\varphi(x)$ is the Gaussian functions of hidden layer, $\varphi(x) = [\varphi_1(x), \varphi_2(x), \dots, \varphi_l(x)]^T \in \mathbb{R}^l$, $\varphi_j(x)$ can be calculated as follows

$$\varphi_j(x) = \exp(-\frac{\|x - \mu_{ij}\|^2}{\eta^2}), \quad i = 1, 2, \dots, q; j = 1, 2, \dots, l.$$

$\mu_{ij}$ and $\eta$ represent the center and width of $\varphi_j(x)$ respectively; $W^* = [w_1, \dots, w_l]^T$ represents the ideal weight vector and it is defined as

$$W^* := arg \min_{\widehat{W} \in \mathbb{R}^l} \{\sup_{x \in \Omega} | f(x) - \widehat{f}(x) | \widehat{W}\},$$

$\widehat{W} = [\widehat{\omega}_1, \dots, \widehat{\omega}_l]^T$ is the output layer weight vector and designed in the next section, $\widetilde{W} = W^* - \widehat{W}$.

In fact, RBF-NN can be used to approximate an arbitrary signal in theoretical. If approximation error $\varepsilon$ trends to zero, the designed RBF-NN can completely reconstruct the malicious abnormal actuator attacks or/and disturbances. In what follows, the reconstructed signal will be used to counteract the adverse effects of the abnormal actuator signal.

## 2.4 | Control Objectives for Networked Path Following of AGVs

In this subsection, the time-delay system modeling is conducted to capture the networked path following of AGVs, which is convenient to stability analysis and synthesis for the studied system.

Referring to Reference[28], the holding interval $[t_k h + \tau_k, t_{k+1} h + \tau_{k+1})$ of the ZOH can be divided as

$$\mho = \bigcup_{n=0}^{t_{k+1} - t_k - 1} \mho_n$$

where $\mho_n = [t_k h + nh + \tau_k, t_k h + nh + h + \tau_{k+1})$, $n = 0, 1, \dots, t_{k+1} - t_k - 1$.

Denoting $\tau(t) = t - t_k h - nh$ for $t \in \mho_n$, the piecewise-linear function $\tau(t)$ satisfies $\dot{\tau}(t) = 1$ and $0 \leqslant \underline{\tau} \leqslant \tau(t) \leqslant \overline{\tau}$, where $\underline{\tau} = min\{\tau_k\}$ is the lower bound of time delay, $\overline{\tau} = h + max\{\tau_k, \tau_{k+1}\}$ is the upper bound of time delay.

Then, based on the definition of $e(nh)$ and $\tau(t)$, the ET-ASC scheme can be designed as

$$u(t) = Kx(t - \tau(t)) - Ke(nh) - \widehat{f}(x), t \in \mho_n \tag{8}$$

where $K$ is the state feedback controller gain to be designed and $\widehat{f}(x)$ is the designed adaptive corrective signal based on RBF-NN.

According to (2), (3) and (8), the neural-based path following system while considering deception attacks we give its ultimate form

$$\begin{cases} \dot{x}(t) = Ax(t) + B[Kx(t - \tau(t)) - Ke(nh) - \widehat{f}(x) + f(x)] + B_\omega w(t) \\ \text{subjects to: Sigmoid-like ETC scheme (4)} \end{cases} \tag{9}$$

where the initial condition of $x(t)$ on $[-\overline{\tau}, 0)$ as $x(t) = \psi(t)$, $\psi(t_0) = x_0$.

Based on the established closed-loop control system (9), the key idea of this paper lies in the following two aspects:

- The abnormal actuator signal can be reconstructed by RBF-NN.
- Adaptive control scheme can be used to counteract the adverse effects of abnormal signal.

Under the Sigmoid-like ETC scheme, the following two goals are expected to fulfill the adaptive security control for the path following control of AGVs.

1. In the case of $w(t) = 0$, the system (9) is asymptotically stable;
2. For any nonzero $w(t) \in \mathcal{L}_2[0, \infty)$ and an $H_\infty$ disturbance attenuation level $\gamma$, $\|y(t)\| \leq \gamma \|w(t)\|$ under zero initial condition.

## 3 | MAIN RESULTS

In this section, the stability criterion and stabilization criterion, as well as adaptive law are provided for the RBF-NN-based ET-ASC scheme for the system (9) subject to malicious actuator signal. Before achieving the main results of this paper, a lemma on the upper bound of the proposed Sigmoid-like ETC scheme is presented at first.

**Lemma 1.** The upper bound threshold of Sigmoid-like event-triggered communication scheme (4) is given by

$$S(t_k h) \leq \frac{\phi_{\sigma,\vartheta}}{\sigma + \vartheta} \tag{10}$$

*Proof.* It can be easily obtained from the monotonicity (5), this completes proof. □

### 3.1 | Stability Analysis Under Sigmoid-like ETC With RBF-NN

**Theorem 1.** For some given positive constants: $\underline{\tau}$, $\overline{\tau}$, $\gamma$, $\phi_{\sigma,\vartheta}$, $\sigma$, $\vartheta$ and $\varrho$, a matrix $K$. If there exist real symmetric matrices $P > 0$, $\Phi > 0$, $R_i > 0$ $(i = 1, 2)$, $Q_j > 0$ $(j = 1, 2)$, $G > 0$, and $U$ with appropriate dimensions satisfy

$$\begin{bmatrix} R_2 & * \\ U & R_2 \end{bmatrix} > 0, \tag{11}$$

$$\Psi = \begin{bmatrix} \Psi_{11} & * \\ \Psi_{21} & \Psi_{22} \end{bmatrix} < 0, \tag{12}$$

where

$$\begin{aligned}
\Psi_{11} = [(1,1) &= PA + A^T P + Q_1 - R_1 - \frac{\pi^2}{4}G, \\
(2,1) &= R_1, (2,2) = Q_2 - Q_1 - R_1 - R_2, \\
(3,1) &= K^T B^T P + \frac{\pi^2}{4}G, (3,2) = R_2 - U, \\
(3,3) &= U + U^T - 2R_2 - \frac{\pi^2}{4}G + \frac{\phi_{\sigma,\vartheta}}{\sigma + \vartheta}\Phi, \\
(4,2) &= U, (4,3) = R_2 - U, (4,4) = -R_2 - Q_2, \\
(5,1) &= -K^T B^T P, (5,3) = -\frac{\phi_{\sigma,\vartheta}}{\sigma + \vartheta}\Phi, \\
(5,5) &= -\Phi + \frac{\phi_{\sigma,\vartheta}}{\sigma + \vartheta}\Phi, \\
(6,1) &= B_\omega^T P, (6,6) = -\gamma^2 I]; \\
\Psi_{21} &= \text{col}\{\underline{\tau} R_1 \mathfrak{X}_1, (\overline{\tau} - \underline{\tau}) R_2 \mathfrak{X}_1, \overline{\tau} G \mathfrak{X}_1, \mathfrak{X}_2\}; \\
\Psi_{22} &= \text{diag}\{-R_1, -R_2, -G, -I\}; \\
\mathfrak{X}_1 &= [A, 0, BK, 0, -BK, B_\omega], \\
\mathfrak{X}_2 &= [0, 0, C, 0, -C, 0].
\end{aligned}$$

The networked path following control system (9) is asymptotically stable with $H_\infty$ performance under ET-ASC scheme (8) with (14) when suffering from arbitrary abnormal actuator signal $f(x)$.

*Proof.* Based on time-delay analysis method[31] and the principle of RBF-NN approximation method[25], we construct a Lyapunov-Krasovskii functional candidate as

$$V(t, x_t) = \sum_{i=1}^{5} V_i(t, x_t), t \in [t_k h + \tau_k, t_{k+1} h + \tau_{k+1}), \tag{13}$$

where

$$V_1(t,x_t)=x^T(t)Px(t),$$
$$V_2(t,x_t)=\int_{t-\underline{\tau}}^{t}x^T(\xi)Q_1x(\xi)d\xi+\int_{t-\overline{\tau}}^{t-\underline{\tau}}x^T(\xi)Q_2x(\xi)d\xi,$$
$$V_3(t,x_t)=\underline{\tau}\int_{t-\underline{\tau}}^{t}\int_{\xi}^{t}\dot{x}^T(\nu)R_1\dot{x}(\nu)d\nu d\xi+(\overline{\tau}-\underline{\tau})\int_{t-\overline{\tau}}^{t-\underline{\tau}}\int_{\xi}^{t}\dot{x}^T(\nu)R_2\dot{x}(\nu)d\nu d\xi,$$
$$V_4(t,x_t)=\overline{\tau}^2\int_{i_kh}^{t}\dot{x}^T(\xi)G\dot{x}(\xi)d\xi-\frac{\pi^2}{4}\int_{i_kh}^{t}[x(\xi)-x(i_kh)]^TG[x(\xi)-x(i_kh)]d\xi,$$
$$V_5(t,x_t)=\frac{1}{\varrho}\widetilde{W}^T\widetilde{W}.$$

Then, by calculating the derivation of $V(t,x_t)$ along the trajectory of system (9) yields

$$\dot{V}_1(t,x_t)=2x^T(t)P\{Ax(t)+B[u(t)+f(x)]+B_\omega\omega(t)\},$$
$$\dot{V}_2(t,x_t)=x^T(t)Q_1x(t)+x^T(t-\underline{\tau})(Q_2-Q_1)x(t-\underline{\tau})-x^T(t-\overline{\tau})Q_2x(t-\overline{\tau}),$$
$$\dot{V}_3(t,x_t)=\underline{\tau}^2\dot{x}^T(t)R_1\dot{x}(t)+(\overline{\tau}-\underline{\tau})^2\dot{x}^T(t)R_2\dot{x}(t)-\underline{\tau}\int_{t-\underline{\tau}}^{t}\dot{x}^T(\xi)R_1\dot{x}(\xi)d\xi-(\overline{\tau}-\underline{\tau})\int_{t-\overline{\tau}}^{t-\underline{\tau}}\dot{x}^T(\xi)R_2\dot{x}(\xi)d\xi,$$
$$\dot{V}_4(t,x_t)=\overline{\tau}^2\dot{x}^T(t)G\dot{x}(t)-\frac{\pi^2}{4}[x(t)-x(t-\tau(t))]^TG[x(t)-x(t-\tau(t))],$$
$$\dot{V}_5(t,x_t)=-\frac{2}{\varrho}\widetilde{W}^T\dot{\widehat{W}}.$$

To find the adaptive law of RBF-NN, we combine (6), (7), (9) and make the following operation

$$\begin{aligned}\dot{V}_1(t,x_t)+\dot{V}_5(t,x_t)&=2x^T(t)P\{Ax(t)+B[u(t)+f(x)]+B_\omega\omega(t)\}-\frac{2}{\varrho}\widetilde{W}^T\dot{\widehat{W}}\\&=2x^T(t)P\{Ax(t)+B[Kx(t_kh)-\widehat{f}(x)+f(x)]+B_\omega\omega(t)\}-\frac{2}{\varrho}\widetilde{W}^T\dot{\widehat{W}}\\&=2x^T(t)P\{Ax(t)+B[Kx(t_kh)+\widetilde{W}^T\varphi(x(t_kh))+\varepsilon]+B_\omega\omega(t)\}-\frac{2}{\varrho}\widetilde{W}^T\dot{\widehat{W}}\\&=2x^T(t)P\{Ax(t)+BK[x(t-\tau(t))-e(nh)]+B_\omega\omega(t)\}+2\widetilde{W}^T(t)[x^T(t)PB\varphi(x(t_kh))-\frac{1}{\varrho}\dot{\widehat{W}}]+2x^T(t)PB\varepsilon.\end{aligned}$$

Then, the adaptive law is given by

$$\dot{\widehat{W}}=\varrho x^T(t)PB\varphi(x(t_kh)). \tag{14}$$

By using Jensen's inequality and convex optimization property[32] to deal with the integral term in $\dot{V}_3(t,x_t)$, this yields

$$-\underline{\tau}\int_{t-\underline{\tau}}^{t}\dot{x}^T(\xi)R_1\dot{x}(\xi)d\xi\le-\begin{bmatrix}x(t)\\x(t-\underline{\tau})\end{bmatrix}^T\begin{bmatrix}R_1&*\\-R_1&R_1\end{bmatrix}\begin{bmatrix}x(t)\\x(t-\underline{\tau})\end{bmatrix} \tag{15}$$

and

$$-(\overline{\tau}-\underline{\tau})\int_{t-\overline{\tau}}^{t-\underline{\tau}}\dot{x}^T(\xi)R_2\dot{x}(\xi)d\xi\le-F^T\begin{bmatrix}R_2&*&*\\U-R_2&2R_2-U^T-U&*\\-U&U-R_2&R_2\end{bmatrix}F \tag{16}$$

where $F^T=[x^T(t-\underline{\tau}),x^T(t-\tau(t)),x^T(t-\overline{\tau})]$, matrix $U$ satisfies $\begin{bmatrix}R_2&*\\U&R_2\end{bmatrix}>0$.

According to Lemma 1, it is clearly that

$$e^T(nh)\Phi e(nh)<\frac{\phi_{\sigma,\vartheta}}{\sigma+\vartheta}x^T(t_kh)\Phi x(t_kh) \tag{17}$$

for $t \in \mho_n$.

By summing up (14)-(17) and applying Schur complement lemma, the following results can be reached

$$\dot{V}(t, x_t) \leq \zeta^T(t)\Psi\zeta(t) + 2x^T(t)PB\varepsilon - y^T(t)y(t) + \gamma^2 w^T(t)w(t) \tag{18}$$

where $\Psi = \Psi_{11} - \Psi_{21}^T\Psi_{22}^{-1}\Psi_{21}$ is defined in (12), $\zeta^T(t) \triangleq [x^T(t), x^T(t-\underline{\tau}), x^T(t-\tau(t)), x^T(t-\overline{\tau}), e^T(nh), w^T(t)]$.

Furthermore, based on (18), one has

$$\zeta^T(t)\Psi\zeta(t) + 2x^T(t)PB\varepsilon \leq \lambda_{max}(\Psi)||\zeta(t)||_F^2 + 2|\overline{\varepsilon}|\lambda_{max}(P)||x(t)||_F \tag{19}$$

where $\lambda_{max}(\diamond)$ represents the maximum eigenvalue of $\diamond$; $||\square||_F^2$ represents the square root of sum of squares of all the elements in $\square$.

In order to guarantee $\dot{V}(t, x_t) \leq 0$, the following inequality should be satisfied

$$\lambda_{max}(\Psi)||\zeta(t)||_F^2 + 2|\overline{\varepsilon}|\lambda_{max}(P)||x(t)||_F \leq 0. \tag{20}$$

Notice that $||\zeta(t)||_F^2 \geq ||x(t)||_F^2 \geq 0$, $\lambda_{max}(\Psi) < 0$, then the convergence radius of $x(t)$ can be obtained

$$||x(t)||_F \geq -\frac{2|\overline{\varepsilon}|\lambda_{max}(P)}{\lambda_{max}(\Psi)}. \tag{21}$$

From the result, it is clear that the convergence radius of $x(t)$ becomes tighter when one obtains smaller $\lambda_{max}(\Psi)$, bigger $\lambda_{max}(P)$ and especially the $\overline{\varepsilon}$ (the maximum of RBF-NN approximation error) is tiny, which means that the system (9) has higher tracing precision.

Next, from (18) to (21), one can see that if the LMI (12) holds, then

$$\dot{V}(t, x_t) \leq \zeta^T(t)\Psi\zeta(t) - y^T(t)y(t) + \gamma^2 w^T(t)w(t). \tag{22}$$

And $V(t, x_t)$ is continuous in $t$, the integration of both sides from 0 to $+\infty$ yields

$$V(+\infty) - V(0) \leq \int_0^{+\infty} [\gamma^2 w^{\mathrm{T}}(\alpha)w(\alpha) - y^{\mathrm{T}}(\alpha)y(\alpha)]d\alpha \tag{23}$$

Under the zero initial condition, the following result we can obtain that

$$\int_0^{+\infty} y^{\mathrm{T}}(\alpha)y(\alpha)d\alpha \leq \gamma^2 \int_0^{+\infty} w^{\mathrm{T}}(\alpha)w(\alpha)d\alpha, \tag{24}$$

i.e., $\|y(t)\| \leq \gamma\|w(t)\|$ holds for any non-zero $w(t) \in \mathcal{L}_2[0, \infty)$.

In the case of $w(t) = 0$, there exists a positive scalar $\epsilon$ such that $\dot{V}(t, x_t) \leq \epsilon\|x(t)\|^2$ for $x(t) \neq 0$ under the condition (11) (12). Then, we can conclude that the system (2) is asymptotically stable with an $H_\infty$ performance. This completes the proof. □

*Remark 4.* The adaptive law (14) contains the real-time system state $x(t)$, which is difficult to obtain directly. In view of practice, we can use the sampled-data $x(t_k h)$ in place of $x(t)$ if the sampling period is very small, i.e., $\widehat{W} = \varrho x^T(t_k h)PB\varphi(x(t_k h))$.

From Theorem 1, it is obvious that only adaptive law of $\widehat{W}$ is obtained while the fixed state feedback controller $K$ is not reached. In what follows, the controller gain $K$ of system (9) will be synthesized according to the sufficient condition of asymptotically stable in Theorem 1.

## 3.2 | RBF-NN-based ET-ASC Design

**Theorem 2.** For some given positive constants $\overline{\tau} > \underline{\tau}$, $\phi_{\sigma,\vartheta}$, $\sigma$, $\vartheta$ and $\gamma$, if there exist real symmetric matrices $X > 0$, $\Phi^\star > 0$, $R_i^\star > 0$, $Q_j^\star > 0$ $(i, j = 1, 2)$, $G^\star > 0$ and $U^\star$, $Y$ with appropriate dimensions satisfy

$$\begin{bmatrix} R_2^\star & * \\ U^\star & R_2^\star \end{bmatrix} > 0, \quad \begin{bmatrix} \Psi_{11}^\star & * \\ \Psi_{21}^\star & \Psi_{22}^\star \end{bmatrix} < 0 \tag{25}$$

where

$$\begin{aligned}
\Psi_{11}^{\star} &= [(1,1) = AX + XA^T + Q_1^{\star} - R_1^{\star} - \frac{\pi^2}{4}G^{\star},\\
&\quad (2,1) = R_1^{\star}, (2,2) = Q_2^{\star} - Q_1^{\star} - R_1^{\star} - R_2^{\star},\\
&\quad (3,1) = Y^T B^T + \frac{\pi^2}{4}G^{\star}, (3,2) = R_2^{\star} - U^{\star},\\
&\quad (3,3) = U^{\star} + U^{\star T} - 2R_2^{\star} - \frac{\pi^2}{4}G^{\star} + \frac{\phi_{\sigma,\vartheta}}{\sigma+\vartheta}\Phi^{\star},\\
&\quad (4,2) = U^{\star}, (4,3) = R_2^{\star} - U^{\star}, (4,4) = -R_2^{\star} - Q_2^{\star},\\
&\quad (5,1) = -Y^T B^T, (5,3) = -\frac{\phi_{\sigma,\vartheta}}{\sigma+\vartheta}\Phi^{\star},\\
&\quad (5,5) = -\Phi^{\star} + \frac{\phi_{\sigma,\vartheta}}{\sigma+\vartheta}\Phi^{\star},\\
&\quad (6,1) = B_{\omega}^T, (6,6) = -\gamma^T I];\\
\Psi_{21}^{\star} &= \mathrm{col}\{\underline{\tau}\mathcal{X}_1, (\overline{\tau} - \underline{\tau})\mathcal{X}_1, \overline{\tau}\mathcal{X}_1, \mathcal{X}_2\};\\
\Psi_{22}^{\star} &= \mathrm{diag}\{-XR_1^{\star -1}X, -XR_2^{\star -1}X, -XG^{\star -1}X, -I\};\\
\mathcal{X}_1 &= [AX, 0, BY, 0, -BY, B_{\omega}],\\
\mathcal{X}_2 &= [0, 0, C, 0, -C, 0].
\end{aligned}$$

Then the system (9) can be stabilized by

$$u(t) = YX^{-1}x(t_k h) - \widehat{f}(x) \tag{26}$$

under Sigmoid-like ETC scheme (4) with an $H_{\infty}$ performance. Here, $\widehat{f}(x) = \widehat{W}^T\varphi(x(t_k h))$ is an estimation of abnormal actuator signal with $\dot{\widehat{W}} = \varrho x^T(t_k h)PB\varphi(x(t_k h))$.

*Proof.* Define $X = P^{-1}$, $Q^{\star} = XQX$, $R^{\star} = XRX$, $U^{\star} = XUX$, $\Phi^{\star} = X\Phi X$, $G^{\star} = XGX$, $Y = KX$, $\Delta_1 = \mathrm{diag}\{X, X, X, X, X, I, R_1^{-1}, R_2^{-1}, G^{-1}, I\}$, $\Delta_2 = \mathrm{diag}\{X, X\}$. Then, pre- and post-multiplying both sides of (11) (12) by $\Delta_1$ and $\Delta_2$. Next, the inequality $-X\diamond^{-1}X \leqslant \rho^2\diamond - 2X$ is used to deal with the above nonlinear items $-XR_i^{\star -1}X$ $(i = 1, 2)$ and $-XG^{\star -1}X$ [33]. This completes the proof. □

In the end of this section, an algorithm is presented to find the controller gain $K$ and event-triggered parameters in (25).

**Algorithm 1** Find the allowable communication parameters $\sigma$, $\vartheta$, $\phi_{\sigma,\vartheta}$, $\Phi$, and the controller gain $K$.

**1:** Initialized the parameters $\sigma$, $\phi_{\sigma,\vartheta}$, $\overline{\tau}$, $\underline{\tau}$, and $\vartheta$ with optimization target $topt < 0$.

**2:** Use the MATLAB LMI Toolbox to solve LMIs (25).

**3:** If there is a feasible solution $X$, $Q^{\star}$, $R^{\star}$ and $\Phi$, go to next step; otherwise, return Step 1.

**4:** $\vartheta = \vartheta + S_{ep}$, where $S_{ep}$ is the increment of $\vartheta$.

**5:** Return $\vartheta$ and the corresponding $K$, $\Phi$ based on Theorem 2.

## 4 | SIMULATION EXAMPLES

In this section, simulation experiments are given to verify the effectiveness of the proposed RBF-NN-based ET-ASC scheme.

Before proceeding further, we detailed the experiment setups as following aspects

- *Vehicle parameters:* $M = 1480kg, v_x = 5m/s, C_f = 62191N/rad, C_r = 98727N/rad, I_z = 2562kg \cdot m^2, l_f = 1.08m, l_r = 1.62m$. The initial state $x_0 = [0.2; 0; 0.1; 0]$.
- *Simulation parameters:* The simulations are set as $h = 0.01s$, $\gamma = 100$, $\underline{\tau} = 0.01s$, $\overline{\tau} = 0.05s$, and $\omega(t) = 0.01e^{-t}$.
- *Event-triggered parameters:* The event-triggered parameters are set as $\sigma = 1$, $\vartheta = 1$ and $\phi_{\sigma,\vartheta} = 0.1$.
- *Malicious signal:* The launched abnormal or disturbance signal is assumed that $f(x) = tanh(x_1(t_k h))$.

By solving the LMIs in Theorem 2, the following results can be easily obtained:

$$K = \begin{bmatrix} 0.0059 & 0.0044 & 0.0726 & -0.0027 \end{bmatrix}, \quad \Phi = 10^4 \times \begin{bmatrix} 0.9968 & -0.3339 & 0.4166 & -0.0786 \\ -0.3339 & 1.9097 & -0.0962 & 0.2222 \\ 0.4166 & -0.0962 & 0.1913 & -0.0339 \\ -0.0786 & 0.2222 & -0.0339 & 1.6410 \end{bmatrix}.$$

In what follows, the comparisons between traditional ETC scheme and the proposed RBF-NN-based ET-ASC scheme are given to illustrate the effectiveness of the proposed approach.

## 4.1 | Traditional ETC Scheme

In this case, we consider the controller without any other auxiliary design, i.e., $u(t) = Kx(t_k h)$. Under the injection of the malicious signal, the actuators will make wrong actions. Clearly, Fig. 3(a) shows that the state response curve is disordered and eventually tends to oscillation, which means that the stability of the system (9) will be lost. Meanwhile, huge amounts of transmissions are released (see Fig. 3(b)). This is because that the event-triggered threshold $S(t_k h)$ is adaptively changed along with the system state (Fig. 3(c)). The control signal is shown in Fig. 3(d) which shows unexpected actions.

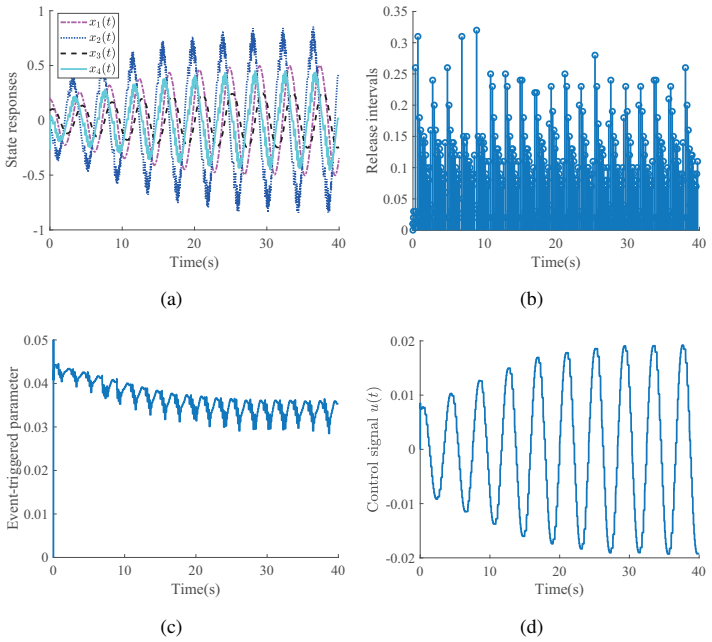


**FIGURE 3** Simulation results of case A: (a) State responses, (b) Released intervals and instants, (c) Evolutions of event-triggered threshold $S(t_k h)$, (d) Control signal.

The above simulation results show that the traditional ETC scheme can not yet stabilize the path following of AGVs when there are malicious actuator signal.

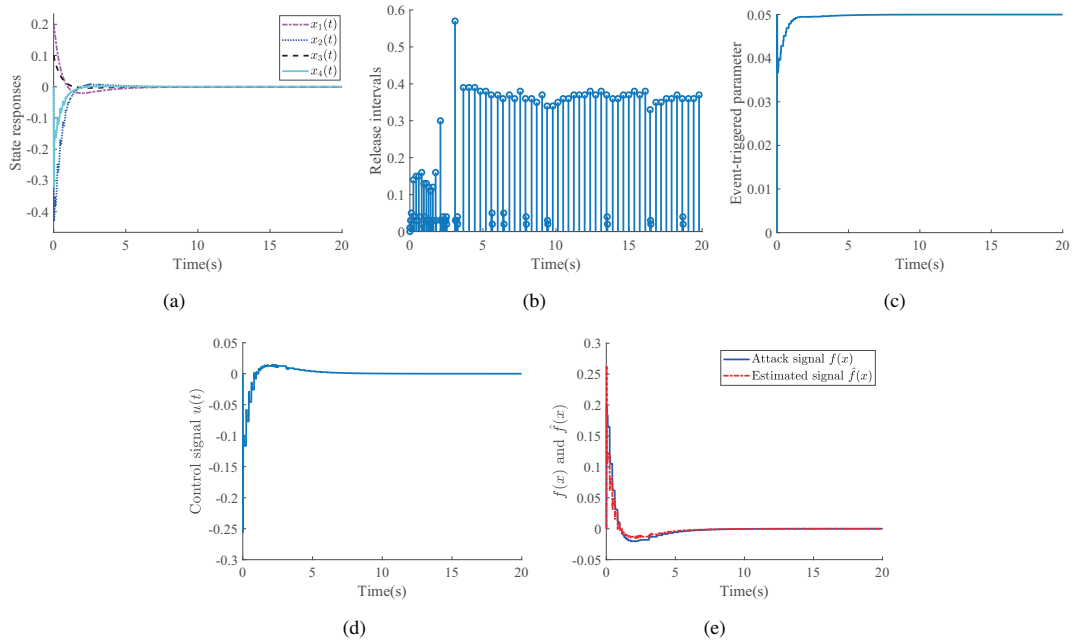


**FIGURE 4** Simulation results of case B: (a) State responses, (b) Release interval and instant, (c) Changes of event-triggered threshold $S(t_k h)$, (d) Changes of controller signal, (e) RBF NN estimated signal $\hat{f}(x)$ approach to $f(x)$.

**TABLE 2** Transmissions and average transmission period under different ETC schemes

| Schemes | ETC threshold | Transmitted packets | Average period | Performance |
|---|---|---|---|---|
| Time-triggered scheme[7] | 0 | 2000 | 0.0100 | Good |
| Static ETC scheme[28] | 0.01 | 310 | 0.0644 | Good |
| | 0.05 | 128 | 0.1564 | Worse |
| | 0.1 | 96 | 0.2065 | Worse |
| Sigmoid-like ETC scheme | $S(t_k h)$ | 110 | 0.1785 | Good |

## 4.2 | RBF-NN-based ET-ASC Scheme

Now, we consider the case of RBF-NN-based ET-ASC scheme. It is not difficult to design the ET-ASC controller with the form of

$$u(t) = Kx(t_k h) - \hat{f}(x)$$

where the adaptive law is derived from

$$\dot{\widehat{W}} = \varrho x^T(t_k h) P B \varphi(x(t_k h)).$$

Let neural network $\widehat{W}^T \varphi(x(t_k h))$ contains $11^4$ nodes such that centers spaced evenly cover the compact set $[-5, 5]^4$ and set $\varrho = 10$. Thus,

$$P = \begin{bmatrix} 0.0001 & -0.0000 & -0.0002 & -0.0000 \\ -0.0000 & 0.0003 & 0.0009 & -0.0003 \\ -0.0002 & 0.0009 & 0.0077 & 0.0001 \\ -0.0000 & -0.0003 & 0.0001 & 0.0006 \end{bmatrix}.$$

The simulation results are given by Fig. 4. From the simulations, the following results can be obtained

1. By comparing Fig. 3(a) and Fig. 4(a), it is clearly that the system (9) can be well stabilized by using the proposed RBF-NN-based ET-ASC scheme.

2. From Fig. 4(b) and Table 2, which show that Sigmoid-like ETC scheme is capable of scheduling communication resources in an adaptive way.

3. Fig. 4(e) shows that RBF-NN can be used to estimate the launched malicious actuator signal in an effective way.

It should be pointed out that the control performance is greatly improved when the controller is equipped with RBF-NN-based estimator. This confirms the effectiveness of the proposed RBF-NN-based ET-ASC scheme.

## 5 | CONCLUSIONS

In this paper, RBF-NN-based ET-ASC scheme has been studied for path following of AGVs under malicious actuator signal. By assuming there are false data injection attacks or/and disturbance signal at actuator side, RBF-NN has been used to estimate such the malicious signal and model-based adaptive control approach has been exploited to secure the stability for networked path following of AGVs. The proposed RBF-NN-based ET-ASC scheme has the adaptive ability in both malicious signal approximation and Sigmoid-like ETC scheme. This guarantees that the proposed scheme is of enchanted security and scheduling ability. Based on the observations of the proposed RBF-NN-based ET-ASC scheme, it integrates with both data-driven feature in RBF-NN approximation and model-based control property in controller design. However, this paper has only considered abnormal signal from actuator side. In the future, a more complicated attack scenario will be investigated.

## ACKNOWLEDGMENTS

This work was partially supported by the National Natural Science Foundation of China (Nos. 62103229, 61833011, 62173218), the Natural Science Foundation of Shandong Province under Grant ZR2021QF026, and the China Postdoctoral Science Foundation under Grant 2021M692024.

### Conflict of interest

The authors declare no potential conflict of interests.

### Data availability statement

Data are available on request from the authors.

## References

1. Wei R, Ella A. Distributed multi-vehicle coordinated control via local information exchange. *Int J Robust Nonlinear Control.* 2007; 17(10–11): 1002–1003.

2. Aguiar A, Hespanha J. Trajectory-tracking and path-following of underactuated autonomous vehicles with parametric modeling uncertainty. *IEEE Trans Autom Control.* 2007; 52(8): 1362–1379.

3. Ji X, Liu Y, He X, et al. Interactive control paradigm-based robust lateral stability controller design for autonomous automobile path tracking with uncertain disturbance: A dynamic game approach. *IEEE Trans Veh Technol.* 2018; 67(8): 6906–6920.

4. Ji J, Khajepour A, Melek W, Huang Y. Path planning and tracking for vehicle collision avoidance based on model predictive control with multiconstraints. *IEEE Trans Veh Technol.* 2017; 66(2): 952–964.

5. Cheng S, Li L, Chen X, Wu J, Wang H. Model-predictive-control-based path tracking controller of autonomous vehicle considering parametric uncertainties and velocity-varying. *IEEE Trans Ind Electron.* 2021; 68(9): 8698–8707.

6. Zeng W, Khalid M, Chowdhury S. In-vehicle networks outlook: Achievements and challenges. *IEEE Commun Surv Tutor.* 2016; 18(3): 1552–1571.

7. Peng C, Li F. A survey on recent advances in event-triggered communication and control. *Inform Sciences.* 2018; 457: 113–125.

8. Yue D, Tian E, Han QL. A delay system method for designing event-triggered controllers of networked control systems. *IEEE Trans Autom Control.* 2013; 58(2): 475–481.

9. Peng C, Han QL. A novel event-triggered transmission scheme and $\mathcal{L}_2$ control co-design for sampled-data control systems. *IEEE Trans Autom Control.* 2013; 58(10): 2620–2626.

10. Peng C, Zhang J, Yan H. Adaptive event-triggering $H_\infty$ load frequency control for network-based power systems. *IEEE Trans Ind Electron.* 2018; 65(2): 1685–1694.

11. Gu Z, Yue D, Tian E. On designing of an adaptive event-triggered communication scheme for nonlinear networked interconnected control systems. *Inform. Sciences* 2018; 422: 257–270.

12. Girard A. Dynamic triggering mechanisms for event-triggered control. *IEEE Trans Autom Control.* 2014; 60(7): 1992–1997.

13. Wang K, Tian E, Liu J, Wei L, Yue D. Resilient control of networked control systems under deception attacks: A memory-event-triggered communication scheme. *Int J Robust Nonlinear Control.* 2020; 30(4): 1534–1548.

14. Gu Z, Yin T, Ding Z. Path Tracking Control of Autonomous Vehicles Subject to Deception Attacks via a Learning-Based Event-Triggered Mechanism. *IEEE Trans Neur Net Lear.* 2021; 32(12): 5644–5653.

15. Sun H, Peng C, Ding F. Self-discipline predictive control of autonomous vehicles against denial of service attacks. *Asian J Control.* 2022: 1–14.

16. Hu S, Yue D, Xie X, Chen X, Yin X. Resilient event-triggered controller synthesis of networked control systems under periodic DoS jamming attacks. *IEEE Trans Cybern.* 2019; 49(12): 4271–4281.

17. Ge X, Han QL, Zhong M, Zhang XM. Distributed Krein space-based attack detection over sensor networks under deception attacks. *Automatica.* 2019; 109: 1–10.

18. Zhang P, Sun H, Peng C, Tan C. Sigmoid-like event-triggered security cruise control under stochastic false data injection attacks. *Processes.* 2022; 10(7): 1–14.

19. Chattopadhyay A, Lam KY, Tavva Y. Autonomous vehicle: Security by design. *IEEE Trans Intell Transp Syst.* 2021; 22(11): 7015–7029.

20. Pasqualetti F, Dorfler F, Bullo F. Control-theoretic methods for cyberphysical security: Geometric principles for optimal cross-layer resilient control systems. *IEEE Control Syst Mag.* 2015; 35(1): 110–127.

21. Gu Z, Park J, Yue D, Wu ZG, Xie X. Event-triggered security output feedback control for networked interconnected systems subject to cyber-attacks. *IEEE Trans Syst Man, Cybern, Syst.* 2021; 51(10): 6197–6206.

22. Ju Z, Zhang H, Tan Y. Deception attack detection and estimation for a local vehicle in vehicle platooning based on a modified UFIR estimator. *IEEE Internet Things J.* 2020; 7(5): 3693–3705.

23. Musleh A, Chen G, Dong Z. A survey on the detection algorithms for false data injection attacks in smart grids. *IEEE Trans Smart Grid.* 2019; 11(3): 2218–2234.

24. Chen FC, Khalil H. Adaptive control of a class of nonlinear discrete-time systems using neural networks. *IEEE Trans Autom Control.* 1995; 40(5): 791–801.

25. Shao X, Ye D. Neural-network-based adaptive secure control for nonstrict-feedback nonlinear interconnected systems under DoS attacks. *Neurocomputing.* 2021; 448: 263–275.

26. Sari A. Turkish national cyber-firewall to mitigate countrywide cyber-attacks. *Comput Electr Eng.* 2019; 73: 128–144.

27. Meng X, Rozycki P, Qiao JF, Wilamowski B. Nonlinear system modeling using RBF networks for industrial application. *IEEE Trans. Industr. Inform.* 2018; 14(3): 931–940.

28. Peng C, Yang T. Event-triggered communication and $H_\infty$ control co-design for networked control systems. *Automatica.* 2013; 49: 1326–1332.

29. Ge X, Ahmad I, Han QL, Wang J, XM Z. Dynamic event-triggered scheduling and control for vehicle active suspension over controller area network. *Mech Sys Signal Pr.* 2021; 152: 1–26.

30. Zhang XM, Han QL, Ge X, et al. Networked control systems: A survey of trends and techniques. *IEEE/CAA J Autom Sinica.* 2020; 7(1): 1–17.

31. Zhang J, Peng C, Du D, Zheng M. Adaptive event-triggered communication scheme for networked control systems with randomly occurring nonlinearities and uncertainties. *Neurocomputing.* 2016; 174(3): 475–482.

32. Park P, Kob J, Jeong C. Reciprocally convex approach to stability of systems with time-varying delays. *Automatica.* 2011; 47: 235–238.

33. Ghaoui L, Oustry F, AitRami M. A cone complementarity linearization algorithm for static output-feedback and related problems. *IEEE Trans Autom Control.* 1997; 42(8): 1171–1176.